THE JOURNAL OF PHYSICAL CHEMISTRY B

Article

pubs.acs.org/JPCB

Structural Spectroscopy and Dynamics of Inter- and Intramolecular H-Bonding Interactions of Topotecan, a Potent Anticancer Drug, in Organic Solvents and in Aqueous Solution

Maria Rosaria di Nunzio, YiLun Wang, and Abderrazzak Douhal*

Departamento de Química Física, Facultad de Ciencias Ambientales y Bioquímica, and INAMOL, Universidad de Castilla−La Mancha, Avenida Carlos III, S/N, 45071 Toledo, Spain

Supporting Information

ABSTRACT: We report on the role of H-bonding interactions on the UV−visible absorption and emission (steady-state and time-resolved) spectroscopy of topotecan (TPT) in solution. In aprotic solvents, a very fast (less than 10 ps) excited-state intramolecular proton-transfer reaction occurs in the absorbing enol (E) form to give a zwitterion (Z) form, emitting with a large Stokes shift. In protic solvents like methanol, the time constant of Z* formation is longer (32 ps) due to the participation of solvent molecules in the proton-transfer reaction. In aqueous solution at near-neutral pH (6.24), a ground-state equilibrium is established between E, cation (C), and Z forms. Direct excitation of E leads to Z* through two channels: a very fast one (less than 10 ps) involving an intramolecular proton-tranfer and a slower one (680 ps) with the C* intermediate formation and reaction. A fast (42 ps) deprotonation of E* to give the excited anion (A*) also competes with the photoformation of Z* at the S_1 state. At pH =12.15, the A structures are the principal emitting species ($\tau_A \sim 0.41$ ns), showing the largest Stokes shift. In aqueous solutions, we cannot exclude the existence of an equilibrium between the lactone and carboxylate forms of TPT, whose spectroscopic (absorption and emission spectra) and dynamical behaviors should not be very different. Time-resolved emission anisotropy measurements in solvents of different viscosities suggest that the rotational relaxation time (φ) of TPT is mainly governed by the viscosity of the medium, increasing from 104 ps (in tetrahydrofuran, THF) to 156 ps (in water) and 338 ps (in dimethyl sulfoxide, DMSO). These results give spectroscopic and dynamical information on the structures, stability, and dynamics (picosecond to nanosecond time scale) of TPT in solution. They provide insights on the role of the intermolecular H-bonding surrounding medium on the ground- and excited-state structure and reaction of TPT. The finding should contribute to a better understanding of the relationship between the structures of the drug and its surroundings.

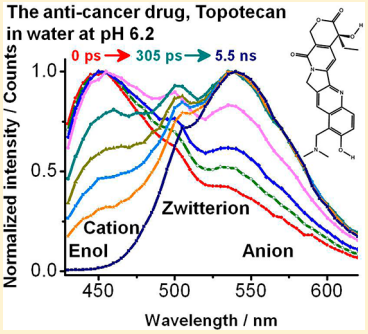

1. INTRODUCTION

Topotecan (TPT) (Scheme 1) is a water-soluble analogue of camptothecin (CPT), which is clinically used in the cancer treatment of ovarian,[1] small-cell lung,[2] and more recently cervical cancers.[3] The mechanism of action of CPT family drugs consists of specifically reducing the activity of the human topoisomerase I (Top1) enzyme through the formation of a Top1−DNA complex.[4−6] The final result is the lethal DNA strand break. The stability of the Top1−DNA complex significantly depends on the nature and strength of the interactions (H-bonding and stacking interactions) between CPTs and the flanking base pairs.[7]

As with the CPT derivatives, TPT undergoes a pH-dependent hydrolysis of the lactone ring to give a relatively inactive and more toxic carboxylate form in aqueous solution (Scheme 1S in Supporting Information).[8,9] To overcome this drawback, inclusion complexes of TPT into liposomes, cyclodextrins (native and hydroxypropylated β-cyclodextrin), and sulfonatocalix[4]arene (SC4A) have been investigated with the aim to retain the drug in its active lactone form, to increase the delivery to tumor sites, and to provide sustained drug release and hence tumor exposure.[10−13] In addition to

Scheme 1. Molecular Structure of TPT in Its Lactone Form

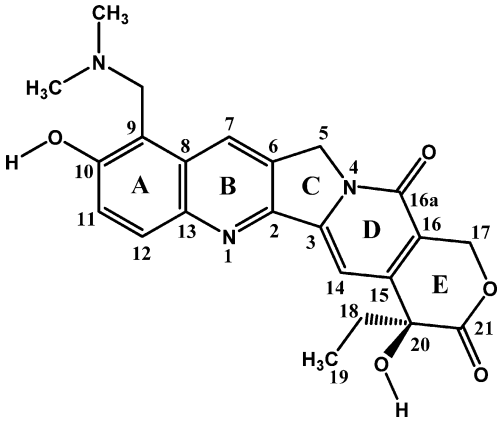

Received: March 27, 2012
Revised: May 28, 2012
Published: June 4, 2012

Scheme 2. Molecular Structures of TPT[a]

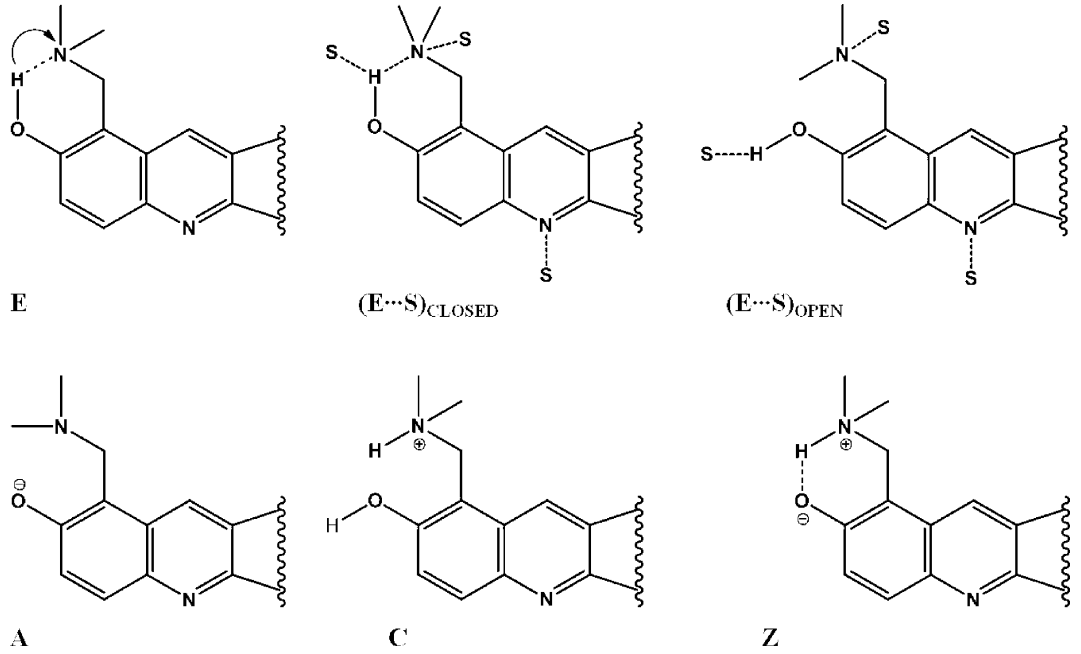

[a]E, enol; $(E\cdots S)_{closed}$ and $(E\cdots S)_{open}$, solvent-H-bonded enol; A, anion; C, cation; Z, zwitterion. For simplicity, only the quinoline moiety is shown.

important effects of the medium pH, light exposure has also been recently reported to affect the pharmacological activity of many promising anticancer, antiviral, and anti-inflammatory drugs.[14−18] To get a basic idea on the possibility of these phenomena and their significance, one can simply look at the molecular structure of these drugs. The basic structure of TPT consists of five rings, of which four (A, B, D, and E) are six-membered and one (C) is five-membered. The H-atoms on the 9- and 10-positions of the A-ring are replaced by dimethylaminomethylene and hydroxyl groups, respectively. The multifunctional nature of the molecule is evidenced by the presence of different kinds of possible interactions with the solvent. More specifically, the presence of the 10-hydroxyl and 9-dimethylaminomethylene groups makes feasible the restoration of different excited-state prototropic processes. On the other hand, quinoline derivatives are well-known to give birth to different excited-state species, including triplet states.[19−22] Therefore, a detailed knowledge of solvent effects on the kind of drug at the S_0 and S_1 states is essential for better drug design, synthesis, stability, and understanding of phototoxicity and role of functional groups. The influence of the medium on the properties of TPT in its ground and electronically first excited states has been mainly investigated by UV−visible absorption and fluorescence (stationary and time-resolved) spectroscopy.[23−29] The equilibria between different forms of the drug were determined at moderately acidic and physiological pH values,[27] and good agreement was achieved between the experimental results and those of theoretical (DFT) calculations.[30] The emission spectrum of TPT is sensitive to solvent polarity.[28] In aqueous buffer solutions, with either one- or two-photon excitation, a single exponential emission decay (τ = 5.9 ns) was observed as the result of an excited-state intramolecular proton-transfer (ESIPT) reaction involving the 9-dimethylaminomethylene and 10-hydroxyl groups. A significant effect of the surrounding on the relaxation of excited TPT was also deduced from the multiexponential emission decay in propylene glycol.[28] However, among the variety of reports on TPT in solution, we found no additional information on its excited-state dynamics in water at different proton concentrations.

Here, we report on steady-state (UV−visible absorption and emission) and time-resolved picosecond (ps) emission studies of TPT in four different organic solvents (tetrahydrofuran, THF; dichloromethane, DCM; acetonitrile, ACN; and methanol, MeOH) and in aqueous solutions at pH 6.24 and 12.15. The obtained results show, for all the studied solvents,multiple emission due to an excited-state proton-transfer (ESPT) reaction that converts the initial absorbing species (enol, E, and/or cation, C) to the respective zwitterion (Z) and/or anion (A) (Scheme 2). The mechanism and, thus, the rate constant of the proton-transfer reaction are strongly affected by the nature of the H-bonds formed between the drug and solvent molecules. The pH-dependent hydrolysis of TPT and, thus, the coexistence of its lactone and carboxylate forms have been also taken into account. These results reflect the influence of the H-bonding surroundings on the ground- and excited-state behavior of TPT, thus providing new insights on drug stability, structures, and photobehavior in different organic solvents and in aqueous solution at two different pH values (6.24 and 12.15).

2. EXPERIMENTAL SECTION

(*S*)-(+)-Topotecan hydrochloride (TPT, ≥98%), anhydrous tetrahydrofuran (THF, ≥99.9%), dichloromethane (DCM, ≥99%), acetonitrile (ACN, ≥99.9%), and anhydrous methanol (MeOH, 99.9%) were from Sigma−Aldrich and were used as received. Deionized water was used to prepare the aqueous solutions. Steady-state absorption and emission spectra were recorded on a Varian (Cary E1) spectrophotometer and a Perkin-Elmer LS 50B spectrofluorometer, respectively. Emission lifetimes were measured by use of a picosecond time-correlated single-photon-counting (TCSPC) spectrophotome-

dx.doi.org/10.1021/jp302923a | J. Phys. Chem. B 2012, 116, 7522−7530

ter (FluoTime 200, PicoQuant) described elsewhere.[31] The sample was excited by a 40 ps pulsed (20 MHz) laser centered at 371 or 433 nm. The instrumental response function (IRF) of the apparatus was typically 65 ps. Fluorescence signal, gated at the magic angle (54.7°), was monitored at a 90° angle to the excitation beam at discrete emission wavelengths by use of a 100 mm monochromator between the sample and the Hamamatsu microchannel plate photomultiplier (R3809-U21). Decay data were analyzed by use of the FluoFit software package (PicoQuant). Exponential decay functions were convoluted with the experimental response function and fit to the experimental decay. The quality of the fits was characterized in terms of the reduced χ^2 value and the distribution of residuals. All the measurements were done at 293 K, and fresh solutions were always used.

3. RESULTS AND DISCUSSION

3.1. Study in Organic Solvents. *3.1.1. Steady-State Observation. 3.1.1.1. UV–Visible Absorption Spectra.* As far as we know, there are no previous UV–visible absorption spectra of TPT in the organic solvents used in this study. Figure 1A shows the recorded spectra. The long-wavelength intensity

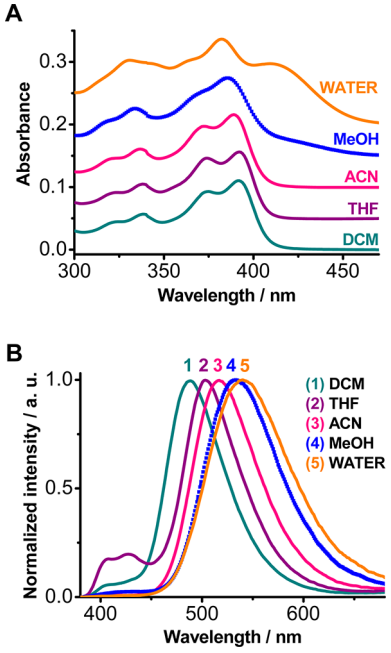

Figure 1. (A) UV–visible absorption spectra of TPT in different organic solvents and in water at pH 6.24. The $S_0 \rightarrow S_1$ absorption bands corresponding to absorption of the quinoline moiety are shown. For clarity, the spectra are shifted along the *y*-axis. (B) Emission spectra (normalized to the maximum of intensity) of TPT in different organic solvents and in water at pH 6.24. The excitation wavelength was 371 nm.

maxima between 350 and 400 nm, corresponding to the $S_0 \rightarrow S_1$ transition, are principally due to the $\pi-\pi^*$-type absorption of the quinoline moiety (A- and B-rings). Figure 1A shows that, for TPT in apolar aprotic (THF, DCM) and polar aprotic (ACN) solvents, the spectral position of the absorption band is not sensitive to the nature of the medium, suggesting that a large molecular population exists as a noninteracting enol (E) form (Scheme 2). We did not observe any ground-state evidence of the zwitterionic (Z, Scheme 2) form of TPT in aprotic solvents. However, in MeOH, H-bonding interactions between the solvent molecules and the D-ring of TPT have the effect of shifting the spectrum to lower wavelengths (by about 6 nm), most probably as a result of reduction in the charge-transfer character, at the excited state, between the carbonyl group and the quinoline moiety.[29] In addition to that, we observe the appearance of a new long-wavelength band around 420 nm, which we assign to the absorption of both the Z and the anion (A, Scheme 2) forms of the drug, formed by strong H-bonding interaction of TPT with methanol molecules. Support for the latter assignment comes from the effect of the alkaline pH (12.15) on the UV–visible absorption and emission spectra in water (see after).

3.1.1.2. Emission Spectra. TPT, dissolved in organic solvents and excited at 371 nm, clearly gives a dual emission (Figure 1B), with a blue fluorescent band in the 385–450 nm range and a green one at longer wavelengths (450–700 nm). The blue band originates from the excited E, while the green band species is the zwitterion, Z*, result of an excited-state intramolecular proton-transfer (ESIPT) reaction between the 10-hydroxyl group and the nitrogen atom on the 9-dimethylaminomethylene group. After its formation, Z* undergoes on S_1 a fast electronic reorganization involving an electron/charge transfer from the deprotonated 10-OH to the D-ring carbonyl groups before relaxing to the ground state (Scheme 1S in Supporting Information). The emission of TPT is sensitive to the solvent.[28] The large Stokes shift value ($\Delta\bar{\nu}$ = 5000–7080 cm^{-1}) for the Z* emission band reflects a large electronic redistribution due to the proton-transfer reaction. Fluorescence excitation spectra of TPT in the various solvents were gated at both the blue and green emission bands (Figure 2A). The results indicate the coexistence of at least two ground-state forms of TPT in these solvents, a red-shifted absorbing species and a blue-shifted one. They are responsible for the

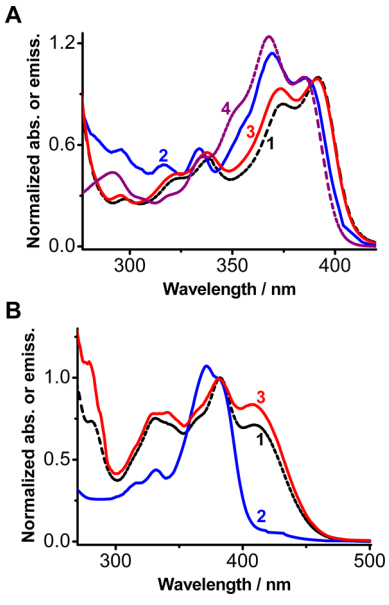

Figure 2. (A) UV–visible absorption (1) and excitation spectra [(2), λ_{em} = 406 nm; (3), λ_{em} = 487 nm] of TPT in DCM, normalized to the maximum of intensity. For comparison, the normalized absorption spectrum of the parent molecule CPT (4) is shown. (B) Normalized UV–visible absorption (1) and excitation spectra [(2), λ_{em} = 425 nm, corresponding to $(E\cdots H_2O)_{open}$; (3), λ_{em} = 580 nm, corresponding to C and Z] of TPT in water at pH 6.24.

dx.doi.org/10.1021/jp302923a | J. Phys. Chem. B 2012, 116, 7522–7530

green and blue emission bands, respectively. The red-shifted absorbing species, whose excitation spectrum is similar to that of the absorption one, is ascribed to E having an intramolecular hydrogenbond (IHB) in aprotic solvents or $(E\cdots S)_{closed}$ structures in MeOH (Scheme 2). In $(E\cdots S)_{closed}$, in spite of the interaction with the protic MeOH, the IHB is still present. However, we assigned the blue-shifted absorbing species to open enol complexes $[(E\cdots S)_{open}$, Scheme 2], where intermolecular H-bonds (iHBs) between TPT and the solvent molecules are formed in disfavor of the IHB one. In addition to these species (closed and open E structures), in MeOH, Z and A species also coexist at the ground state. It is important to note that Z and A forms originate from closed and open E structures, respectively. Thus, the proton transfer reaction from the 10-OH group to water (to give A) does not compete with the proton transfer between the 10-OH group and the 9-dimethylaminomethylene (to give Z) because they occur in different species. Upon excitation at 433 nm, where only Z and A absorb, we did not observe any displacement of the green emission maximum with respect to that obtained from excitation at 371 nm (data not shown). This result suggests that most of the Z* emission comes from direct excitation of Z, whose population at S_0 is in large excess with respect to the A one. The emission lifetime experiments also support this suggestion (vide infra, section 3.1.2).

3.1.2. Picosecond Time-Resolved Emission Measurements. For a better understanding of the interactions of excited TPT with the various solvents, we recorded the picosecond emission decays upon excitation at 371 and 433 nm (the latter only in MeOH). Representative results of TPT in THF, MeOH, and water, with excitation at 371 nm and gating at both blue and red sides of the emission spectrum, are shown in Figure 3A, B. Table 1 gives the obtained time constants (τ_i) and normalized pre-exponential factors (A_i) from a multiexponential fit of the signals (λ_{exc} = 371 and 433 nm, the latter only for water solutions). Other wavelengths have been also examined (Supporting Information, Tables 1S–5S). The lifetime constants were accurately determined from a global analysis of the decays at several observation wavelengths ($\chi^2 \leq 1.1$). The results clearly indicate that the excited-state photorelaxation of TPT is sensitive to solvent properties (H-bonding ability and polarity). The results in water solutions will be discussed later in section 3.2.2. In ACN, a polar and aprotic solvent, short ($\tau_1 \sim 70$ ps, $\tau_2 = 1.37$ ns) and long ($\tau_3 \sim 5$ ns) components were determined. The former components mainly contribute in the 410–490 nm region ($A_1 = 68\%$, $A_2 = 20\%$ at 410 nm), while the latter one ($A_3 = 12\%$ at 410 nm) becomes the only component at longer wavelengths (516–620 nm region). In less polar and aprotic solvents, like THF and DCM, we still observe a long and red-emitting component ($\tau_3 = 5.08$ ns in THF and 4.59 ns in DCM, with A_3 close to 100% for $\lambda_{obs} > 500$ nm), while in the blue band only one short time constant ($\tau_2 = 2.61$ and 2.38 ns for THF and DCM, respectively) is observed. We assign τ_2 to excited $(E\cdots S)_{open}$, while τ_3 corresponds to Z*. The origin of the fast component, τ_1, found in ACN is ascribed to an excited solvated complex interacting with the solvent molecules, probably at both its acid (10-hydroxyl) and basic (9-dimethylaminomethylene, N1 atom) groups. The difference in the lifetime values of blue and green fluorescence indicates that there is no equilibrium between the E* and Z* forms in the excited state. The limited picosecond time resolution of the apparatus (~10 ps after deconvolution of the signal with an IRF of 65 ps), does not allow us to observe a rising picosecond component (below 10 ps) in the emission decay of Z*. Moreover, the dimerization process of TPT, occurring even at low concentrations ($\sim 2 \times 10^{-5}$ M),[27] did not make feasible the use of femtosecond (fs) time-resolved emission spectroscopy, due to the high optical densities needed to carry out such experiments. Ultrafast ESIPT reactions usually occur in less than 100 fs.[32] In hydrogen-bonding solvents (MeOH), the excited-state dynamics are slowed down with respect to that found in aprotic solvents, as has been observed in another H-bonding system.[33] Upon excitation at 371 nm, the 32-ps component represents a decay in the 440–520 nm region ($A_1 = 77\%$ at 440 nm) and a rise in the green one ($A_1 = -22\%$ at 600 nm), which indicates that the excited $(E\cdots CH_3OH)_{closed}$ structure undergoes a fast dynamics (in the picosecond time domain) to produce Z*. The value of the rate constant for the excited-state intermolecular proton-transfer (ESiPT) reaction of TPT in MeOH is $k_{ESiPT} = 1/\tau_1 = 3.12 \times 10^{10}$ s^{-1}. The produced Z* has a lifetime τ_3 of ~5.6 ns. Its contribution in the blue emission is very low ($A_3 = 1\%$ at 440 nm), reaching its maximum value (91%) at 540 nm (around the emission intensity maximum of the steady-state fluorescence spectrum). The assignation of τ_3 to Z* was further confirmed upon excitation at 433 nm, where the largest population of TPT is in the Z form. A major component (τ_2 =

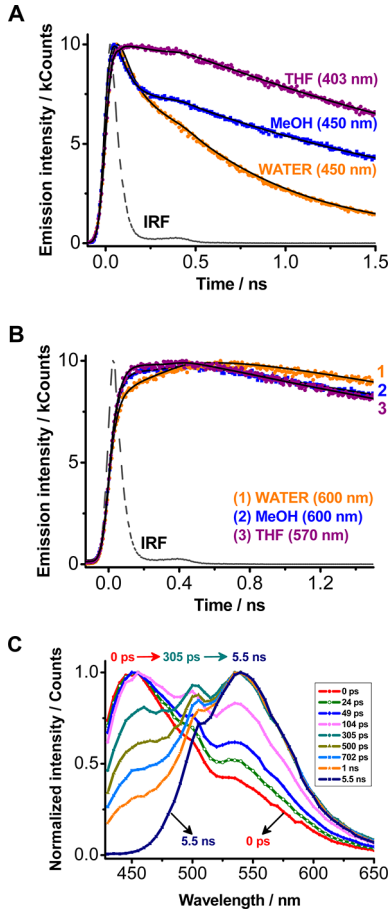

Figure 3. Emission decays of TPT in water at pH 6.24, MeOH, and THF gated (A) in the blue (403, 450 nm) and (B) red (570, 600 nm) sides of the fluorescence emission signal. Solid lines are from the best exponential fit. (C) Normalized magic-angle time-resolved emission spectra (TRES) of TPT in water at pH 6.24, gated at the indicated delay times after excitation at 371 nm. (Inset) Gating times of the spectra.

dx.doi.org/10.1021/jp302923a | J. Phys. Chem. B 2012, 116, 7522–7530

Table 1. Values of Fluorescence Time Constants and Normalized Pre-exponential Factors of Fitting Decay Functions for TPT in Organic Solvents and in Water at Different pH Values[a]

solvent	λ_{em}, nm	τ_1, ps (A_1, %)	τ_2, ns (A_2, %)	τ_3, ns (A_3, %)
		λ_{ex} = 371 nm		
THF	403		2.61 (94)	5.08 (6)
THF	600		2.61 (2)	5.08 (98)
DCM	406		2.38 (91)	4.59 (9)
DCM	620			4.59 (100)
ACN	410	69 (68)	1.37 (20)	4.96 (12)
ACN	620			5.00 (100)
MeOH	440	32 (77)	1.44 (22)	5.02 (1)
MeOH	600	32 (−22)		5.73 (78)
H_2O, pH6.24	450	42 (52)	0.68 (46)	5.77 (2)
H_2O, pH 6.24	600	42 (−20)	0.68 (−5)	5.76 (75)
H_2O, pH 12.15	500		0.40 (75)	3.66 (25)
H_2O, pH 12.15	650		0.40 (98)	3.66 (2)
		λ_{ex} = 433 nm		
H_2O, pH 6.24	460		0.63 (8)	5.80 (92)
H_2O, pH 6.24	620			5.80 (100)
H_2O, pH 12.15	530		0.41 (92)	3.63 (8)
H_2O, pH 12.15	680		0.41 (98)	3.63 (2)

[a]Excitation wavelengths were 371 and 433 nm (the latter only for water solutions). The emission was gated at different wavelengths (λ_{em}).

5.74 ns, $A_2 \geq 94\%$), very close to that found upon excitation at 371 nm, was obtained at all wavelengths of observation (Supporting Information, Table 5S). The minor component (τ_1 = 0.54 ns, $A_1 \leq 6\%$), contributing mostly at lower energies, is assigned to the emission of directly excited A. A lifetime of ∼1.5 ns was obtained for the open structure, $(E\cdots CH_3OH)_{open}$*. Due to the low protolytic photodissociation rate in neat MeOH,[34] the formation of A* from $(E\cdots CH_3OH)_{open}$* was not observed under our experimental conditions. For the parent compound, 10-hydroxycamptothecin (10-CPT), the rate constant of intermolecular ESPT, which is low in neat MeOH, increases with the molar fraction of water in MeOH/water mixtures.[15] The results is explained in terms of (1) preferential solvation of the hydroxyl group by water and (2) gradual change in the solvation energy of the contact ion pair.

In summary, the nature of the organic solvent (polarity, H-bond-donating acidity, H-bond-accepting basicity, and polarity/polarizability) plays a role in both the absorption and emission (steady-state and picosecond time-resolved) properties of TPT. Weak and strong intermolecular H-bonds between the drug and solvent molecules can be formed, giving birth to different ground-state structures. The picosecond time-resolved emission studies show that the rates of inter- and intramolecular proton-transfer reactions depend on the nature and strength of the intermolecular H-bonds in these species. In aprotic, less interacting solvents, the excited-state dynamics occur on a very short (<10 ps) time scale, while in methanol, for example, a slower time (32 ps) is observed due to a proton relay where solvent molecules play a role in the tautomer formation, as has been observed for bifunctional molecules.[35−38]

3.2. Study in Water Solutions. *3.2.1. Steady-State Observation. 3.2.1.1. UV−Visible Absorption Spectra.* Figure 1A shows the UV−visible absorption spectrum of TPT at pH 6.24. Due to the presence of multifunctional groups, TPT has been already reported to undergo several equilibria between different structures depending on the pH of the solution.[27] In particular, four pK_a values have been experimentally determined: pK_{a1} < 0.8 and pK_{a2} ∼ 3.6, assigned to the protonation of N1 and N4 sites, respectively; and pK_{a3} = 6.5 and pK_{a4} = 10.7, relative to the deprotonation of 10-hydroxyl and protonated 9-dimethylaminomethylene groups, respectively (Supporting Information, Table 6S). Protonation of the D-ring at the N4 site (in the 2.64−4.56 pH range) does not significantly affect the absorption spectrum of the quinoline moiety of TPT, because of the low conjugation between the A-, B-, and D-rings. Quantum chemical calculation results agree with the experimental titration data.[30] On the basis of the above pK_a values, we propose the following structures of TPT in equilibrium at pH 6.24: enol [$(E\cdots H_2O)_{open}$, λ_{abs}^{max} = 374 nm], cation (C, λ_{abs}^{max} = 382 nm), and zwitterion (Z, λ_{abs}^{max} = 409 nm), as shown in Scheme 2. Table 2 reports their spectroscopic

Table 2. Steady-State UV−Visible Absorption and Fluorescence Data for Various Forms of TPT

form of TPT	absorption bands λ_{max}, nm ($\bar{\nu}_{max}$, 10^3 cm^{-1})	experimental (theoretical) data from literature[a]	emission bands λ_{max}, nm ($\bar{\nu}_{max}$, 10^3 cm^{-1})
E, enol	374[b] (26.74)		421[c] (23.75)
C, cation	382, 331, 268 (26.18, 30.21, 37.31)	382 (352), 327 (301), 267 (249), 223 (220)	455[d] (21.98)
A, anion	420 (23.81)		556 (17.99)
Z, zwitterion	409, 344, 281 (24.45, 29.07, 35.59)	412 (420), 340 (351), 282 (272), 227 (223)	540 (18.52)

[a]From ref 27. [b]From the excitation spectrum (425 nm). [c]From deconvolution with a two-Gaussian-component fitting algorithm. [d]From TRES.

data. The C species shows protonation on the 9-dimethylaminomethylene group, the latter showing a pK_a value (pK_{a4} = 10.7) higher than the pH (6.24) of the water, while $(E\cdots H_2O)_{open}$ is ascribed to E in an open configuration interacting with water molecules through intermolecular H-bonds (iHBs). In Z, whose ground-state structure is the same as that assigned for TPT in MeOH, a salt bridge involves the 10- and 9-substituents. The existence of such a bond facilitates the retention of proton at the 9-dimethylaminomethylene group and thus increases its pK_a value. At this proton concentration, the ground-state equilibrium does not involve the anionic form (A), which becomes the prevailing species (λ_{abs}^{max} = 420 nm, Scheme 2 and Figure 1S in Supporting Information) only in highly alkaline conditions (pH = 12.15). The scarce contribution of A to the ground-state population of TPT forms at pH 6.24 is also suggested from the emission lifetime experiments (vide infra, section 3.2.2). CPT family drugs contain an additional hydroxyl group at the 20-position on the E-ring. The nonaromatic nature of the latter should ensure a higher pK_a value for deprotonation of the hydroxyl group at the 20-position with respect to that at the 10-position, due to less stability of the deprotonated E-ring compared to that of the

dx.doi.org/10.1021/jp302923a | J. Phys. Chem. B 2012, 116, 7522−7530

deprotonated A-ring. Thus, we can exclude the lactone ring ionization at pH 6.24.

As has been previously mentioned, aqueous solutions of CPTs undergo a hydrolysis of the lactone E-ring to give a relatively inactive and more toxic carboxylate form (pK_a of carboxylic group ~6.5).[8,9] The rate constant of the hydrolysis reaction of aqueous CPT mostly depends on the pH, increasing as the proton concentration decreases.[8,9] The half-life ($t_{1/2}$) of the lactone form of CPT in homogeneous phosphate buffer solutions at 37 °C is ~17 min.[39] Substitution of a hydroxyl group at the 10-position, as in 10-hydroxycamptothecin and 7-ethyl-10-hydroxycamptothecin derivatives, has the effect of stabilizing the lactone form, increasing its $t_{1/2}$ up to 22 min.[39] For 10-hydroxycamptothecin derivatives in water and water/MeOH mixtures, it has been shown by the use of steady-state (UV−visible absorbance and emission spectra, circular dichroism) and time-resolved (pump−probe and fluorescence) measurements that E-ring hydrolysis does not practically modify the ground- and excited-state behavior.[15] By use of the equilibrium constant value (K_{eq} = 0.4) reported at 298 K for the hydrolysis of TPT in aqueous solution at pH 6,[40] we estimate that ca. 30% of TPT lactone form is hydrolyzed in our conditions (pH = 6.24). On the basis of these considerations, we do not disregard the existence of an equilibrium between the lactone and carboxylate forms (E, C, or Z; Scheme 1S in Supporting Information) in water at near-neutral pH, as it has been also supported by TD-DFT calculations.[30] However, if they coexist, they should not have very different spectroscopic (absorption and emission spectra) and kinetic behaviors. We did not observe any spectral change when a 2-day-old solution of TPT in phosphate buffer at pH = 7.44 was studied again, thus evidencing that the lactone and carboxylate forms show very similar absorption (and emission, vide infra) patterns.

3.2.1.2. Emission Spectra. At pH 6.24, we observed the typical emission from Z* ($\Delta\bar{\nu}_{ST(Z^*)}$ ~ 7660 cm^{-1}) as shown in Figure 1B (pH 6.24). On the other hand, the emission intensity from the blue-emitting E* is very weak. By use of a Gaussian-type peak function (Supporting Information, Figure 2S), we deconvoluted the spectra and get a maximum intensity at λ_{em}^{max} of 421 nm for the emission spectrum of E* in water at pH 6.24. A normal Stokes shift value [$\Delta\bar{\nu}_{ST(E^*)}$ = 2425 cm^{-1}] is then observed, being very close to that found in MeOH [$\Delta\bar{\nu}_{ST(E^*)}$ ~ 2380 cm^{-1}]. The ground-state equilibrium between $(E\cdots H_2O)_{open}$, C, and Z forms at pH 6.24, as previously discussed, is supported by analysis of the excitation spectra (Figure 2B). Here, both the C and Z forms clearly contribute to the green emission, while the blue one originates mostly from the E species. Good agreement was found between the experimental (UV−visible) and calculated[27] wavelengths of the absorption intensity maxima for C [382 (352), 331 (301), and 268 (249)] and Z [409 (420), 344 (351), and 281 (272)] forms. As was discussed before, the contribution of A to the total ground-state absorption is very weak and can be ignored, as this was confirmed by the fact that Z* was observed as the main emitting fluorophore even upon excitation at 433 nm (data not shown). The emission of A* is observed in alkaline solution (pH = 12.15) upon excitation at 371 or 433 nm. It displays a band centered at 556 nm with a Stokes shift [$\Delta\bar{\nu}_{ST(A^*)}$ = 8190 cm^{-1}; Supporting Information, Figure 1S]. At this high pH, we expect that A is totally hydrolyzed.[40] The excitation spectrum of A is similar to that of the absorption one (data not shown). No change in the emission spectrum was detected when a fresh solution of TPT in phosphate buffer (pH = 7.44) was studied again after 2 days in the dark.

In summary, due to the different sites in the TPT frame, there are three main possible chemical structures in equilibrium in aqueous solution at pH 6.24: cation, enol, and zwitterion. The contribution of A to the total ground-state absorption is very weak. The Z* form is the main emitting fluorophore under these conditions.

3.2.2. Picosecond Time-Resolved Emission Measurements. The picosecond emission experiments of TPT in water at pH 6.24 were carried out with excitation at 371 and 433 nm. Figure 3 shows the emission decays of TPT in water at pH 6.24 upon excitation at 371 nm (where mainly E and C forms absorb) and gated at short (450 nm, A) and long (600 nm, B) emission wavelengths. Table 1 collects the obtained time constants (τ_i) and normalized pre-exponential factors (A_i) for the fits by use of multiexponential functions in a global analysis. More details are given in the Supporting Information, Tables 9S and 10S. For excitation at 371 nm, three components were required to fit the decays (Table 1 and Supporting Information, Table 9S). Short decaying components (τ_1 = 42 ps and τ_2 = 0.68 ns) were observed in the 450−500 nm region. The first has its maximum contribution in the blue side of the emission signal (A_1 = 52% at 450 nm), while the second contributes mostly at 500 nm. Both τ_1 and τ_2 components are rising at lower energies of the emission, with absolute contributions ($|A_i|$%) being maxima at 620 and 530 nm for τ_1 and τ_2, respectively. The long component, τ_3 = 5.76 ns, is decaying at all wavelengths of observation, with the maximum A_3 value in the green emission band (530 nm). On the basis of the pK_a^* values of the different functional groups of TPT (Supporting Information, Table 6S), we assign the 42-ps component to deprotonation of directly excited $(E\cdots H_2O)_{open}$ at the 10-hydroxyl group (pK_{a3}^* = −2.62, ΔpK = −9.12). The generated A* relaxes to S_0 with a lifetime of 0.41 ns (observed at pH 12.15; Table 1 and Supporting Information, Tables 7S and 8S). We did not observe this time in the emission decay because it is masked by the presence of a rise, in the same region, of the 680-ps component. However, as the pK_a^* value of the 9-dimethylaminomethylene group is higher than that at the ground state (pK_{a4}^* = 13.15, ΔpK = 2.45), protonation of this group is also possible, and it occurs on a fast time scale (<10 ps) that is below the time resolution of the instrumental apparatus. The photoproduced cation (C*) undergoes, during its lifetime (0.63 ns), a slow deprotonation (680 ps) of the 10-OH group to give Z* as the final photoproduct. Direct excitation of C and, in a lesser amount, Z can also occur in these conditions.

Time-resolved emission spectra (TRES) of TPT at pH 6.24 upon excitation at 371 nm, normalized at the intensity maxima, are illustrated in Figure 3C. Fast (subnanosecond time scale) and slower (nanosecond time scale) dynamics of the involved excited species emerge from analysis of the spectral evolution at different time delays in the 430−485 nm region (where the E* and C* forms emit) and at longer wavelengths (where emission comes from Z* and A*), respectively. Fast growth (within the picosecond laser pulse) of the signal from both C* (λ_{em}^{max} = 455 and 500 nm) and Z* (λ_{em}^{max} = 540 nm) supports the formation of C* on a short time scale and also suggests a fast channel for the formation of Z*, where the precursor should be an E* form in a closed and more reactive configuration. Evolution from C* to Z* is observed at delay times >100 ps. The complete disappearance of the emission from both E* and C* forms at longer gating times, while the signal from Z*

dx.doi.org/10.1021/jp302923a | J. Phys. Chem. B 2012, 116, 7522−7530

Scheme 3. Schematic Illustration of Ground- and Excited-State Behavior of TPT in Water at pH 6.24[a]

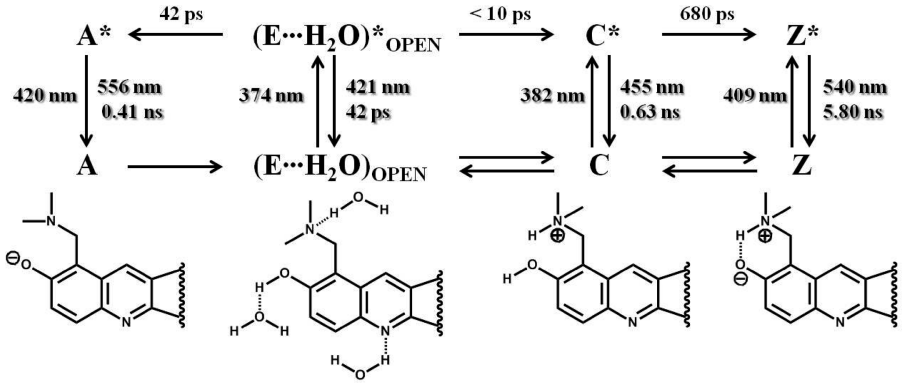

[a]The molecular structures of the involved species [$(E\cdots H_2O)_{open}$, C, Z, and A], with only the quinoline moiety for simplicity, are shown. Excitation was at 371 nm

(λ_{em}^{max} = 540 nm) is still detectable, confirms the absence of the equilibrium at S_1. The observation of different deprotonation rates for $(E\cdots H_2O)^*_{open}$ and C* forms suggests that the proton-transfer reaction depends on the nature of the excited structure and, thus, on its interaction with the water molecules in terms of H-bond making and breaking dynamics.[15] The proton hopping time has been estimated to be 1.7 ps from the bulk proton diffusion constant and 1.3 ps from NMR measurements.[41] Thus, the rate of back proton-transfer from the water molecules can significantly affect the deprotonation of the species [$(E\cdots H_2O)^*_{open}$ or C*] involved in the proton-transfer event. In the enolic form, the significant electron-withdrawing effect exerted from the pyridone D-ring contributes to increase to a great extent the acidity of the 10-hydroxyl group at S_1, thus explaining the fast rate (1/42 ps^{-1}) of deprotonation to give A. The presence of a positive charge on the 9-dimethylaminomethylene group in C* induces an increase in electron density on the A-ring. As a consequence, the excited-state acidity of the 10-hydroxyl group for excited C is reduced (pK_a* for the deprotonation of C* = 1.05, calculated from the Förster cycle;theSupporting Information) and the formation of Z* from C* proceeds in a slowest way due to competition with the back-protonation reaction, which now becomes efficient. Excitation at 433 nm, where Z is the main absorbing species, provides a unique lifetime of 5.80 ns in the 500−700 nm region, while in the blue (460−480 nm) region, a small contribution (3−8%) with a lifetime of 0.63 ns is also observed (Supporting Information, Table 10S). This confirms the previous assignment made for Z* and C* forms. We observed the same dynamics for a solution of TPT in a phosphate buffer (pH = 7.44) after 2 days in the dark.

Summarizing this part (Scheme 3), in aqueous solution at pH 6.24, the S_1 dynamics of TPT is characterized by bi- or triexponential fluorescence decays, depending on the excited species, as ground-state equilibria are established between enol (E), cation (C), and zwitterion (Z) forms (τ_{E^*} = 42 ps, τ_{C^*} = 0.63 ns, τ_{Z^*} = 5.80 ns). The excited-state proton transfer reaction is irreversible, with time constants going from femtosecond to picosecond time domains (τ_{ESPT} = <10 ps, 42 ps, and 680 ps). For alkaline solution at pH = 12.15, the emission comes mainly from A* (τ_{A^*} = 0.41 ns).

3.3. Viscosity Effect on Rotational Time of TPT. To get information on the rotational times (φ) of TPT in solutions, and therefore on its friction with the solvation shell, we performed time-resolved emission anisotropy [$r(t)$] measurements in THF, water, and DMSO, which have different viscosities ($\eta_{20\ °C}$ = 0.49, 1.00, and 2.47 for THF, water, and DMSO, respectively). Figure 4 shows representative $r(t)$ decays. They exhibit monoexponential behavior, and the obtained φ value increases from 104 ps (THF) to 156 ps (water) to 338 ps (DMSO) (Table 3). By modeling TPT as a prolate ellipsoid, nonhydrated rotor, and using Stokes−Einstein−Debye hydrodynamics theory,[42,43] we got orientation relaxation times in THF, water, and DMSO of 82, 152, and 341 ps and 16, 29, and 65 ps under stick- and slip-boundary condition limits, respectively. The expected values under stick conditions are closer to the experimental ones, suggesting that a solvation shell is interacting with TPT. As is expected from the theory,[42,44] the friction reflected by viscosity of the surrounding has the effect of slowing down the rotational motion of the drug. The inset of Figure 4 shows the change of φ with the solvent viscosity (η). The dashed curve is a fit (R = 0.997, slope = 119 ± 4, intercept = 42 ± 7) that supposes a linear change of φ with η. This indicates that the rotational relaxation time of TPT is mainly governed from the viscosity of the medium. A nonzero intercept, with a physical significance not well

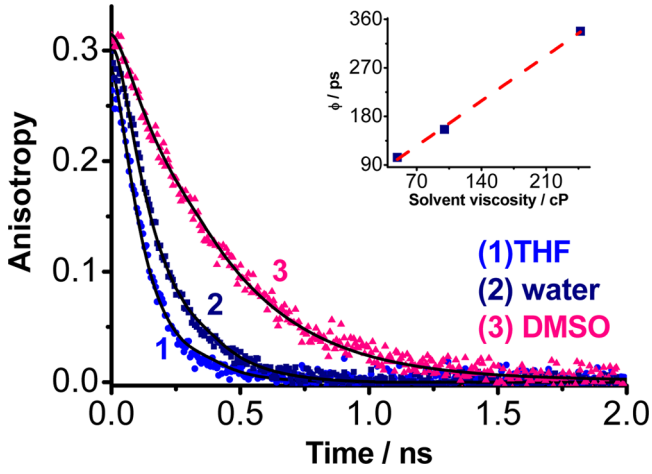

Figure 4. Decays of emission anisotropy of TPT in (1) THF, (2) water at pH 6.24, and (3) DMSO. Solid lines are from the best exponential fit. The excitation wavelength was 371 nm. Observation wavelengths were (1) 505, (2) 530, and (3) 520 nm. (Inset) Change of rotational time constant (φ) as a function of solvent viscosity (η). The dashed curve is a fit that supposes a linear change of φ with η.

dx.doi.org/10.1021/jp302923a | J. Phys. Chem. B 2012, 116, 7522−7530

Table 3. Values of Rotational Times (φ) and Initial Anisotropy (r_0) Obtained from Monoexponential Fits of the Anisotropy Decays [$r(t)$] of TPT Emission in the Indicated Media[a]

	experimental			theoretical	
solvent (λ_{em})	viscosity (20 °C), cP	φ, ps	r_0	τ_{stick}	τ_{slip}
THF (505 nm)	0.49	104	0.28	82	16
water (530 nm)	1.00	156	0.30	152	29
DMSO (520 nm)	2.47	338	0.33	341	65

[a]Excitation wavelength was 371 nm. Observation wavelengths (λ_{em}) are indicated in the table. Comparison with the theoretical orientation relaxation times, calculated under both stick- and slip-boundary condition limits, is also reported in the table.

established yet, has been found previously in other molecules.[45−47] To conclude, an estimation of the angle (~20°) between the emission transition moment of TPT and that of its absorption was made from the initial value of $r(t)$ (r_0 = 0.30), different from the ideal one (0.4), suggesting a very fast emission depolarization due to the proton-transfer reactions, as has been observed in previous reports.[48,49]

4. CONCLUSIONS

The results described and discussed in this work reveal the rich structural dynamics of the anticancer drug TPT in organic solvents (THF, DCM, ACN, and MeOH) and in aqueous solutions at two different pH values (6.24 and 12.15). In all the studied solvents, the drug shows dual emission due to an efficient proton-transfer reaction that converts the enol (E) form to the respective zwitterion (Z). A solvatochromic effect is observed for the emission of Z*. The rate of the proton-transfer reaction is strongly affected by H-bonds formed between the drug and the solvent. In aprotic and less polar solvents (THF, DCM, and ACN) the ESIPT process occurs on a very short (<10 ps) time, proceeding through the IHB between the 10- and 9-groups of the molecule. In the protic solvent MeOH, the time constant of Z* formation is larger (~32 ps) due to participation of solvent molecules in the proton-transfer event. Due to the multifunctional nature of TPT, there are at least four possible chemical structures detectable in aqueous solution at pH 6.24: cation (C), neutral (E), zwitterion (Z), and anion (A) forms. Formation of Z* occurs from directly excited E in less than 10 ps, through an intramolecular proton-tranfer. Moreover, a slower channel (680 ps) of photoformation of Z*, with C* intermediate formation and reaction, also occurs in these conditions. The anion (A, τ_A ~ 0.41 ns), whose contribution to the total ground-state absorption is very low at pH 6.24, dominates at higher pH values (pH = 12.15). In aqueous solutions, the pH-dependent hydrolysis of TPT lactone form to give the carboxylate cannot be disregarded. The UV−visible absorption and emission spectra as well as the emission lifetime behaviors of the two species should not be very different. The rotational relaxation time (φ) of TPT increases from 104 ps (THF) to 156 ps (water) to 338 ps (DMSO), suggesting that it mainly depends on the viscosity of the medium interacting with the molecule in the first solvation shell. We believe that these results provide information on the role of the H-bonding surroundings on both structural and dynamical properties of TPT at its S_0 and S_1 states. This should lead to a better understanding of the relationship between the structure of the drug and the nature of its surroundings as well as its activity with biologically relevant systems (like Top1−DNA).

■ ASSOCIATED CONTENT

Supporting Information

Two figures showing steady-state measurements (absorption and emission spectra) of TPT in alkaline solution and Gaussian deconvolution of the emission spectrum of TPT at pH 6.24; 10 tables listing time-resolved picosecond measurements (upon excitation at 371 and 433 nm) of TPT in the solvents used in this work and ground- and excited-state pK_a values of TPT and their assignation; one scheme showing structures of the enol (E), cation (C), anion (A), and zwitterion (Z) forms of TPT; and additional text describing determination of the excited-state pK_a. This material is available free of charge via the Internet at http://pubs.acs.org.

■ AUTHOR INFORMATION

Corresponding Author

*E-mail Abderrazzak.Douhal@uclm.es; fax +34-925-268840; phone +34-925-265717.

Notes

The authors declare no competing financial interest.

■ ACKNOWLEDGMENTS

This work was supported by the MICINN through project MAT2008-01609. M.R.d.N. and Y.W. thank CYCLON Network (MRTN-CT-2008-Project 237962) for the Marie Curie fellowship.

■ REFERENCES

(1) Sehouli, J.; Oskay-Özcelik, G. Current role and future aspects of topotecan in relapsed ovarian cancer. *Curr. Med. Res. Opin.* **2009**, *25*, 639−651.

(2) Nicum, S. J.; O'Brien, M. E. R. Topotecan for the treatment of small-cell lung cancer. *Expert Rev. Anticancer Ther.* **2007**, *7*, 795−801.

(3) Idris, T.; Winter, R.; Lang, U.; Petru, E. Topotecan-induced long-term remission of an advanced endometrial cancer after treatment with cisplatinum, an anthracycline and paclitaxel. *Anticancer Res.* **2009**, *29*, 1761−1762.

(4) D'Arpa, P.; Liu, L. F. Topoisomerase-targeting antitumor drugs. *Biochim. Biophys. Acta, Rev. Cancer* **1989**, *989*, 163−177.

(5) Pommier, Y. Topoisomerase I inhibitors: Camptothecins and beyond. *Nat. Rev. Cancer* **2006**, *6*, 789−802.

(6) Pommier, Y.; Pourquier, P.; Fan, Y.; Strumberg, D. Mechanism of action of eukaryotic DNA topoisomerase I and drugs targeted to the enzyme. *Biochim. Biophys. Acta, Gene Struct. Expression* **1998**, *1400*, 83−106.

(7) Siu, F. M.; Che, C. M. Persistence of camptothecin analog−topoisomerase I−DNA ternary complexes: A molecular dynamics study. *J. Am. Chem. Soc.* **2008**, *130*, 17928−17937.

(8) Rivory, L. P.; Robert, J. Molecular, cellular, and clinical aspects of the pharmacology of 20(S)camptothecin and its derivatives. *Pharmacol. Ther.* **1995**, *68*, 269−296.

(9) Du, W. Towards new anticancer drugs: A decade of advances in synthesis of camptothecins and related alkaloids. *Tetrahedron* **2003**, *59*, 8649−8687.

(10) Underberg, W. J. M.; Goossen, R. M. J.; Smith, B. R.; Beijen, J. H. Equilibrium kinetics of the new experimental antitumour compound SK and F 104864-A in aqueous solution. *J. Pharm. Biomed. Anal.* **1990**, *8*, 681−683.

(11) Foulon, C.; Tedou, J.; Queruau Lamerie, T.; Vaccher, C.; Bonte, J. P.; Goossens, J. F. Assessment of the complexation degree of camptothecin derivatives and cyclodextrins using spectroscopic and

separative methodologies. *Tetrahedron: Asymmetry* **2009**, *20*, 2482−2489.
(12) Wang, G. S.; Zhang, H. Y.; Ding, F.; Liu, Y. Preparation and characterization of inclusion complexes of topotecan with sulfonato-calixarene. *J. Inclusion Phenom. Macrocyclic Chem.* **2011**, *69*, 85−89.
(13) Tardi, P.; Choice, E.; Masin, D.; Redelmeier, T.; Bally, M.; Madden, T. D. Liposomal encapsulation of topotecan enhances anticancer efficacy in murine and human xenograft models. *Cancer Res.* **2000**, *60*, 3389−3393.
(14) Das, K.; Smirnov, A. V.; Wen, J.; Miskovsky, P.; Petrich, J. W. Photophysics of hypericin and hypocrellin A in complex with subcellular components: Interactions with human serum albumin. *Photochem. Photobiol.* **1999**, *69*, 633−645.
(15) Solntsev, K. M.; Sullivan, E. N.; Tolbert, L. M.; Ashkenazi, S.; Leiderman, P.; Huppert, D. Excited-state proton transfer reactions of 10-hydroxycamptothecin. *J. Am. Chem. Soc.* **2004**, *126*, 12701−12708 and references therein.
(16) El-Kemary, M.; Gil, M.; Douhal, A. Relaxation dynamics of piroxicam structures within human serum albumin protein. *J. Med. Chem.* **2007**, *50*, 2896−2902.
(17) Gil, M.; Douhal, A. Femtosecond dynamics of piroxicam structures in solutions. *J. Phys. Chem. A* **2008**, *112*, 8231−8237.
(18) Cohen, B.; Angel Organero, J.; Santos, L.; Rodriguez Padial, L.; Douhal, A. Exploring the ground and excited states structural diversity of levosimendan, a cardiovascular calcium sensitizer. *J. Phys. Chem. B* **2010**, *114*, 14787−14795.
(19) Itoh, M.; Adachi, T.; Tokumura, K. Time-resolved fluorescence and absorption spectra and two-step laser excitation fluorescence of the excited-state proton transfer in the methanol solution of 7-hydroxyquinoline. *J. Am. Chem. Soc.* **1984**, *106*, 850−855.
(20) Poizat, O.; Bardez, E.; Buntinx, G.; Alain, V. Picosecond dynamics of the photoexcited 6-methoxyquinoline and 6-hydroxyquinoline molecules in solution. *J. Phys. Chem. A* **2004**, *108*, 1873−1880.
(21) Kwon, O. H.; Kim, T. G.; Lee, Y. S.; Jang, D. J. Biphasic tautomerization dynamics of excited 7-hydroxyquinoline in reverse micelles. *J. Phys. Chem. B* **2006**, *110*, 11997−12004.
(22) Angulo, G.; Organero, J. A.; Carranza, M. A.; Douhal, A. Probing the behavior of confined water by proton-transfer reactions. *J. Phys. Chem. B* **2006**, *110*, 24231−24237.
(23) Fassberg, J.; Stella, V. J. A kinetic and mechanistic study of the hydrolysis of camptothecin and some analogues. *J. Pharm. Sci.* **1992**, *81*, 676−684.
(24) Dey, J.; Warner, I. M. Charge-transfer effects on the fluorescence spectra of 9-aminocamptothecin: Steady-state and time-resolved fluorescence studies. *J. Photochem. Photobiol. A: Chem.* **1998**, *116*, 27−37.
(25) Nabiev, I.; Fleury, F.; Kudelina, I.; Pommier, Y.; Charton, F.; Riou, J. F.; Alix, A. J. P.; Manfait, M. Spectroscopic and biochemical characterisation of self-aggregates formed by antitumor drugs of the camptothecin family: Their possible role in the unique mode of drug action. *Biochem. Pharmacol.* **1998**, *55*, 1163−1174.
(26) Chauvier, D.; Chourpa, I.; Maizieres, M.; Riou, J. F.; Dauchez, M.; Alix, A. J. P.; Manfait, M. E-ring conformation has a key role in cleavable complex formation: Homocamptothecin versus camptothecins. *J. Mol. Struct.* **2003**, *651*−*653*, 55−65.
(27) Strel'tsov, S. A.; Grokhovskii, S. L.; Kudelina, I. A.; Oleinikov, V. A.; Zhuze, A. L. Interaction of topotecan, DNA topoisomerase I inhibitor, with double-stranded polydeoxyribonucleotides. 1. Topotecan dimerization in solution. *Mol. Biol.* **2001**, *35*, 365−373.
(28) Gryczynski, I.; Gryczynski, Z.; Lakowicz, J. R.; Yang, D.; Burke, T. G. Fluorescence spectral properties of the anticancer drug topotecan by steady-state and frequency domain fluorometry with one-photon and multi-photon excitation. *Photochem. Photobiol.* **1999**, *69*, 421−428.
(29) Posokhov, Y.; Biner, H.; Içli, S. Spectral-luminescent and solvatochromic properties of anticancer drug camptothecin. *J. Photochem. Photobiol. A: Chem.* **2003**, *158*, 13−20.
(30) Sanna, N.; Chillemi, G.; Grandi, A.; Castelli, S.; Desideri, A.; Barone, V. New hints on the pH-driven tautomeric equilibria of the topotecan anticancer drug in aqueous solutions from an integrated spectroscopic and quantum-mechanical approach. *J. Am. Chem. Soc.* **2005**, *127*, 15429−15436.
(31) Organero, J. A.; Tormo, L.; Douhal, A. Caging ultrafast proton transfer and twisting motion of 1-hydroxy-2-acetonaphthone. *Chem. Phys. Lett.* **2002**, *363*, 409−414.
(32) Douhal, A.; Lahmani, F.; Zewail, A. H. Proton-transfer reaction dynamics. *Chem. Phys.* **1996**, *207*, 477−498.
(33) Douhal, A.; Sanz, M.; Tormo, L.; Organero, J. A. Femtochemistry of inter- and intramolecular hydrogen bonds. *ChemPhysChem* **2005**, *6*, 419−423.
(34) Solntsev, K. M.; Huppert, D.; Agmon, N.; Tolbert, L. M. Photochemistry of "super" photoacids. 2. Excited-state proton transfer in methanol/water mixtures. *J. Phys. Chem. A* **2000**, *104*, 4658−4669.
(35) Mehata, M. S.; Joshi, H. C.; Tripathi, H. B. Steady state and time-resolved spectroscopic studies of 7-hydroxyquinoline in various polymeric matrices. *Spectrochim. Acta, Part A* **2002**, *58*, 1589−1598.
(36) Kohtani, S.; Tagami, A.; Nakagaki, R. Excited-state proton transfer of 7-hydroxyquinoline in a non-polar medium: Mechanism of triple proton transfer in the hydrogen-bonded system. *Chem. Phys. Lett.* **2000**, *316*, 88−93.
(37) Park, S. Y.; Jang, D. J. Accumulated proton-donating ability of solvent molecules in proton transfer. *J. Am. Chem. Soc.* **2010**, *132*, 297−302.
(38) Mehata, M. S.; Joshi, H. C.; Tripathi, H. B. Excited-state intermolecular proton transfer reaction of 6-hydroxyquinoline in protic polar medium. *Chem. Phys. Lett.* **2002**, *359*, 314−320.
(39) Burke, T. G.; Zihou, M. Ethyl substitution at the 7 position extends the half-life of 10-hydroxycamptothecin in the presence of human serum albumin. *J. Med. Chem.* **1993**, *36*, 2580−2582.
(40) Underberg, W. J. M; Goossen, R. M. J.; Smith, B. R.; Beijnen, J. H. Equilibrium kinetics of the new experimental antitumour compound SK&F 104864-A in aqueous solution. *J. Pharm. Biomed. Anal.* **1990**, *8*, 681−683.
(41) Woutersen, S.; Bakker, H. J. Ultrafast vibrational and structural dynamics of the proton in liquid water. *Phys. Rev. Lett.* **2006**, *96*, 138305.
(42) Hu, C.-M.; Zwanzig, R. Rotational friction coefficients for spheroids with the slipping boundary condition. *J. Chem. Phys.* **1974**, *60*, 4354−4357.
(43) Baskin, J. S.; Zewail, A. H. Molecular structure and orientation: Concepts from femtosecond dynamics. *J. Phys. Chem. A* **2001**, *105*, 3680−3692.
(44) Perrin, F. Mouvement Brownien d'un ellipsoide-I. Dispersion diélectrique pour des molécules ellipsoidales. *J. Phys. Radium* **1934**, *5*, 15.
(45) Horng, M. L.; Gardecki, J. A.; Maroncelli, M. Rotational dynamics of coumarin 153: Time-dependent friction, dielectric friction, and other nonhydrodynamic effects. *J. Phys. Chem. A* **1997**, *101*, 1030−1047.
(46) Burdzinski, G.; Buntinx, G.; Poizat, O.; Toele, P.; Zhang, H.; Glasbeek, M. Femtosecond studies of orientational anisotropy decay of benzopyranthione in the excited S2 state in hydrocarbons. *Chem. Phys. Lett.* **2004**, *392*, 470−475.
(47) Anderton, R. M.; Kauffman, J. F. Temperature-dependent rotational relaxation of diphenylbutadiene in *n*-alcohols: A test of the quasihydrodynamic free space model. *J. Phys. Chem.* **1994**, *98*, 12117−12124.
(48) Zhong, D.; Douhal, A.; Zewail, A. H. Femtosecond studies of protein-ligand hydrophobic binding and dynamics: Human serum albumin. *Proc. Natl. Acad. Sci. U.S.A.* **2000**, *97*, 14056−14061.
(49) Douhal, A.; Sanz, M.; Tormo, L. Femtochemistry of orange II in solution and in chemical and biological nanocavities. *Proc. Natl. Acad. Sci. U.S.A.* **2005**, *102*, 18807−18812.